"Development of an impedimetric DNA-biosensor based on layered double hydroxide for the detection of long ssDNA sequences". Baccar, Z. M., Caballero, D., Eritja, R., Errachid, A. Electrochim. Acta, 74, 123-129 (2012).

Development of an Impedimetric DNA-Biosensor Based on Layered Double Hydroxide for the Detection of Long ssDNA Sequences

Z.M. Baccar[1*], D. Caballero[2], R. Eritja[3,4], A. Errachid[5]

[1] Nanobioengineering Group, National Institute of Research and Physicochemical Analysis (INRAP), BiotechPôle de Sidi Thabet, 2020 Sidi Thabet, TUNISIA

[2] Nanobioengineering group-IBEC, Barcelona Science Park, and Department of Electronics, University of Barcelona C/ Baldiri Reixach 10-12, E-08028 Barcelona, SPAIN

[3] Institute for Advanced Chemistry of Catalonia (IQAC-CSIC), Networking Centre on Bioengineering, Biomaterials and Nanomedicine (CIBER-BBN), Jordi Girona 18, E-08034 Barcelona. SPAIN

[4] Institute for Research on Biomedicine (IRB Barcelona), Scientific Parc of Barcelona (PCB), Baldiri Reixac 10, E-08028 Barcelona, SPAIN.

[5] Laboratory of Analytical Sciences (LSA)-UMR 5180, University Claude Barnard of Lyon I, 43 Bd du 11 Novembre 1918, 69622 Vileurbanne Cedex, FRANCE

Corresponding author: zouhair_baccar@topnet.tn

Abstract:

DNA testing requires the development of sensitive and fast devices to measure the presence of nucleic acid sequences by DNA hybridization. In this paper, a simple and label-free DNA-biosensor has been investigated based on the detection of DNA hybridization on layered double hydroxide (LDH) nanomaterials with special emphasis on targeting long single stranded DNA sequences. First, the immobilization of a 20 bases long DNA probe on a thin layer of Mg_2AlCO_3 and Mg_3AlCO_3 LDH was studied. Then, DNA hybridization reaction was detected by means of Electrochemical Impedance Spectroscopy. The resulting biosensor showed a high sensitivity for the detection of 80 bases long DNA complementary sequences. The dynamic range was 18-270 ng/ml with a detection limit lower than 1.8 ng/ml.

Keywords: DNA–biosensor, nanomaterials, layered double hydroxide, self-assembly

1. Introduction

The development of nanomaterials for the immobilization of biomolecules such as nucleic acids and enzymes has attracted great attention in the past decades for the fabrication of chemical sensors [1,2]. The methods of immobilization should respect the conformation of biomolecules in order to maintain the activity and their catalytic performance. In this aim, it is important to develop nanomaterials and suitable methods of immobilization for biomolecules that offer a high affinity for bioreceptors and do not affect the active sites of biomolecules respecting their native conformation. To this end, Layered Double Hydroxide (LDH) nanomaterials are considered as suitable host nanosheets for immobilizing, encapsulating or intercalating biomolecules as well as many other uses [3].

In the past decades, Layered Double Hydroxide nanomaterials have received an attracted interest from industry and scientific community [3]. In fact, LDH are anionic clay with ionic lamellar compounds that consist of positively charged hydroxide sheets and interlayers filled with anions and water [4,5]. They can be represented by the general formula $M^{2+}_{1-x}M^{3+}_{x}(OH)_2\,A^{n-}_{x/n}\,mH_2O$, where M^{2+} are divalent cations (Mg^{2+}, Zn^{2+}, Co^{2+}, Ni^{2+}); M^{3+} are trivalent cations (Al^{3+}, Cr^{3+}, Fe^{3+}) and A^{n-} is an interlayer anion (Cl^-, NO^-_3 , CO^{2-}_3 , SO^{2-}_4) compensating for the charge on the layers [6]. These layered nanomaterials have received high attention due to their versatile properties and their flexibility in bi-dimensional nanomaterial synthesis. They have multiple applications in different fields, such as in catalysis [7], gene and molecular reservoir [8,9], optical materials [10], functional hybrid nanostructured materials [11], controlled drug-release system [12] and thin films [13-16]. Recently, LDH were used as a biomembrane into electrodes for biosensing. The method of immobilization of enzymes and bi-enzymes onto LDH nanosheets [17-20] have permitted the development of biosensors based on simple or multiple metabolic reactions of the analytes.

The immobilization process is based on the ability of the hydroxyl, amine or thiols groups of the biomolecules to cross link with of the metals oxide carrier of the LDHs producing covalent links. The enzymes immobilized onto LDH show high activity and good performance stability [17,19-20].

There is a demand for low-cost portable DNA sensors for biomedical purposes [21]. Label-free electrical detection of nucleic acids may fulfill this demand if a robust and universal system for the immobilization of DNA probes is developed [22]. Electrochemical devices based on the use of 15-30 nucleotide (nt) DNA probes are commonly used [21-23]. These are of interest for the analysis of single mutation in DNA. Alternatively electrochemical DNA sensors may found a large interest in the rapid determination of infectious diseases and bacterial contamination on food. In these cases the analytical target is the presence of long RNA or DNA fragments coming directly from natural sources or after an amplification step such as polymerase chain reaction (PCR). Recently the detection of a 120 nt DNA fragment from avian influenza virus was described using conventional electrochemical impedance spectroscopy on gold disk electrodes [24].

The present paper describes the development of a DNA biosensor for long single-stranded (ss) DNA molecules based of LDH biomembranes. The DNA-sensing performances of the DNA functionalized LDH membranes (sensitivity, dynamic range, and detection limit as well as stability during storage) were studied by electrochemical impedance spectroscopy and a response model was proposed. A high sensitivity of the impedimetric biosensor to the hybridization of the 80-bases long complementary ss oligonucleotide sequence was obtained with a response of 286.7 and 238.5 Ω /ng.ml^{-1} (corresponding to 9.13 and 7.595 kΩ.cm^{-1}/ng.ml^{-1}) at respectively 65 °C and 37 °C. The dynamic range found was from 18 to 270 ng/ml and the detection limit was lower than 1.8 ng/ml.

2. Experimental

2.1 Apparatus and measurements

Powder X-Ray Diffraction (XRD) measurements were performed on a Panalytical X'Pert Pro diffractometer, using CoKα radiation (λ=0.178901 nm) at 40 kV, 30 mA, and continued scanning mode. The scanning rate was 0.16°/s from 7 to 80° -2θ°.

Absorbing Infrared Fourier Transformed (FTIR) spectra in Attenuated Total Reflection (ATR) mode were recorded using an EQUINOX 55 (Bruker) spectrophotometer in the range of 4000–600 cm^{-1} with 2 cm^{-1} resolution and averaging 128 scans.

The morphological characterization of LDH and ODN/LDH samples was performed using a commercial Dimension 3100 AFM (Veeco Instruments, USA), in air at room temperature with a relative humidity of 30 %. The measurements were performed in Tapping^{TM} mode, using a rectangular silicon AFM tip with a spring constant of 3.5 Nm^{-1} and a resonant frequency of 75 kHz (Mikromasch NSC18/AlBS).

The Electroctrochemical impedance spectroscopy (EIS) measurements were performed using voltalab PGZ301 potentiostat from Radiometer Analytical (France). A conventional three-electrode cell assembly consisting of working electrode WE, an SCE reference electrode and a Pt counter electrode CE were used for the electrochemical measurements. The effective area of the WE and the CE electrodes were 0.03 cm^2. All electrochemical experiments were carried out in phosphate buffer 20 mM, 0.275 M of NaCl (pH 7.4) at 37 °C and 65 °C. The frequency range of 100 mHz-100 kHz without polarization and an amplitude of 20 mV. After each series of measurements, the sensor was regenerated by using a basic solution 0.1 M NaOH and stored in PBS at 4 °C.

2.2 DNA probes

Oligonucleotide sequences were prepared on an automatic Applied Biosystems DNA synthesizer mod 3400 using standard protocols and they were purified by reverse phase HPLC using DMT-on and DMT-off protocols. Oligonucleotide sequences carrying an amino and thiol group at the 5'-end were assembled on a 1 μmol scale. Long oligonucleotides were prepared using low volume supports on 200 nmols scale (LV200). The benzoyl (Bz) group was used for the protection of the amino group of C and A, and the isobutyryl (ibu) group for the protection of G. The phosphoramidite derivative of 6-aminohexanol carrying the monomethoxytrityl group (Link Technologies) was used for the introduction of the amino group at the 5'-end. The thiol group at the 5'-end was introduced using the phosphoramidite derivative of 6-hydroxyhexyldisulfide protected with the dimethoxytrityl group (5' thiol modifier C6 S-S CE phosphoramidite (Link Technologies). These DNA sequences were used previously for the assembly of a DNA-templated nanogap electrode [25].

The sequences of thiol, and amino terminated probes were: 20 down-SH: 5'-SH-$(CH_2)_6$-CGA GTC ATT GAG TCA TCG AG-3' and 20 down-NH_2: 5'-NH_2-$(CH_2)_6$-CGA GTC ATT GAG TCA TCG AG-3'. The unmodified 20 down sequence was: 5'-CGA GTC ATT GAG TCA TCG AG-3'.

The sequence of the long DNA probes were: 100 up: 5'-CTA CGT CGC TGA CTA CCT GCG TAG GTC CCT AGA TGG CTA ACT CGG TGC ATC GCT CAC TGG ATA CAT CAG TCC ATG AAT GAC TCG ATG ACT CAA TGA CTC G-3'; 80 down target sequence: TCA TTC ATG GAC TGA TGT ATC CAG TGA GCG ATG CAC CGA GTT AGC CAT CTA GGG ACC TAC GCA GGT AGT CAG CGA CGT AG 3'; negative control DNA sequence 100 NC: 5'- TGC TTT ACG GCA CCT CGA CCC CAA AAA ACT TGA TTA GGG TGA TGG TTC ACG TAG TGG CCA TCG CCC TGA TAG ACG GTT TTT CGC CCT TTG ACG TTG GAG T -3'.

2.3 Fabrication of the Insulator / Semiconductor (IS) samples

The manufacturing process for planar devices was performed at Centro National de Microelectrónica (CNM) of CSIC. The electrodes used in this work are 1cmx1cm substrate sample of $Si_3N_4/SiO_2/Si$<p-type> structure. Their insulator / semiconductor (IS) samples are performed in 100mm diameter wafers of <100>-oriented p-SiO_2 with resistivity of 4-40 Ω cm. The process started with a thermal oxidation process to grow a silicon dioxide layer (SiO_2 78 nm) on silicon wafers in a hydrox furnace at 950 ºC. Then an LPCVD Si_3N_4 layer (100 nm) was deposited on the silicon dioxide at 800 ºC.

2.4 LCD synthesis and ODN/ LDH biomembranes preparation

2.4.1 LDH synthesis

Hydrotalcite (Mg_xAlCO_3) LDH, were prepared by co-precipitation at constant pH and temperature as described [14, 18, 19, 26]. We mixed small amounts (approx. 40 µl) of solutions of $AlCl_3$ and $MgCl_2$ 0.1 M with volume ratio of 1:x at room temperature and at pH 8.0. The pH is maintained constant by addition of a mixed solution of NaOH 2 M and Na_2CO_3 0.125 M. The final precipitates were filtered, washed with MilliQ water, and then dried 12 hours at 100 °C. The resulting solid was crushed in a mortar.

2.4.2 ODN/LDH electrode modification

The biomembranes were deposited in two steps (Figure 1):

* First, a thin layer of LDH was deposited on the Si_3N_4 substrate previously cleaned with Piranha solution (3:7 v/v H_2O_2:H_2SO_4). For this objective, a drop of LDH was previously dispersed in PBS solution (20 mM, pH 7.4), 0.275 M NaCl. Then, it was spin coated at 1000 rpm (10 sec) and 4000 rpm (30 sec) obtaining a thin and uniform layer.

* Secondly, a volume of 5-10 µl of ODN (20 down) was deposited on the surface, at room temperature and in a saturated atmosphere with PBS for 90 minutes. Then, we rinsed the sample with PBS and dried it very carefully with nitrogen.

3. Results and Discussion

The aim of this work is the development of a biosensor for detecting DNA based on LDH biomembranes. The preparation of the sensor consists of the following steps: First LDH biomembranes were prepared and a thin layer of LDH was deposited by spin-coating onto the transducer. Second, the immobilization of a self-assembled layer of a 20 bases DNA probe on a thin layer of LDH biomembranes was achieved. Then a 100 bases long oligonucleotide was hybridized to the 20 bases amino-oligonucleotide immobilized to the LDH membrane obtaining an efficient capture system for the complementary 80 bases long DNA sequence.

3.1 Structural characterization of LDH by X-ray diffraction

Hydrotalcite (Mg_xAlCO_3) LDH, were prepared by co-precipitation at constant pH and temperature as described [14, 18, 19, 26]. Figure 2 shows the X-ray diffractograms of LDHs prepared by co-precipitation. The diffractograms obtained for the synthesized hydrotalcites are in agreement with those reported in the literature (Ross et al 1967 [27]). The phase and structure of these materials were consistent with a crystalline form and an hexagonal crystallization system. However, we note the asymmetry in the peaks of the third, fourth and fifth order. This asymmetry does not correspond to defects in the structure but to an excellent crystallization of the basal charge CO_3^{2-} [28-30].

3.2 Surface analysis of biomembranes by infrared (IR) spectroscopy

3.2.1 ODN/LDHs biomembranes

The comparison of the IR spectra in ATR mode of the ODN/Mg_xAl biomembranes with those of host matrices (Figure 3), allowed us to have an overview of the interaction ODN / LDHs. Figure 3 shows the IR spectra of Mg_xAl biomembranes before and after the addition of 5'NH_2-ODN. The IR spectra of the samples that contain DNA have several signals around 800-1200 cm^{-1} that are due to the aromatic and phosphate groups of the DNA. Similarly, the spectra of different prepared hybrid materials showed peaks between 1340 cm^{-1} and 1239 cm^{-1} and a peak at 1350 cm^{-1}. They correspond to the aromatic amine group of the DNA and the later is associated with the tertiary CH group of DNA, respectively.

The DNA/hydrotalcites (MgAl) hybrid materials show the presence of a peak at 1712 cm^{-1} which corresponds to carbonyl groups. Other peaks appear between 1340 cm^{-1} and 1407 cm^{-1} that may correspond to the carbonyl group of the nucleobases.

3.2.2 Influence of the terminal group at the 5'-end position of the DNA probes

We have studied by infrared spectroscopy in ATR mode (reflection) the surfaces of the biomembranes (ODN-/LDH) and the influence of the amine or thiol functional groups at their 5'-end depending on the mode of immobilization. This technique allowed us to establish the possible interactions between the LDH and the ODN and select the most appropriate end for its anchorage.

For this purpose, we immobilized on Mg_2AlCO_3 membrane two other ODN membranes: one without any functional group and the other with a thiol group at its 5'-SH. The comparative study of the resulting IR spectra (in differential mode: subtraction spectra ODN / LDH and LDH) shows that in the case of ODN without or with 5'-SH the observed oscillations are almost the same (figure 4). The main observed oscillations are specific to the ODN 1061 cm^{-1},

1246 cm^{-1} and 3000-2850 cm^{-1} associated with the free amino groups of the probe. This allows us to suggest that in both cases the immobilization is performed through the bases and the phosphate backbone of the ODN. In this case, the hybridization reaction is difficult because the conformation of the ODN seems to be bent or lying on the layer of LDH difficulting the hybridization. On the other hand, this is not the case with an amine end. For this reason we believe that the amine functional group of the ODN is important as anchoring point which respects the optimal conformation for the hybridization reactions.

3.3 Atomic force microscopy (AFM) characterization

3.3.1 ODN/LDHs morphology

Figure 5.a shows an example of the topography of thin layer of LDH. As it can be observed, the LDH layer was uniformly distributed on the substrate forming a very thin layer with a RMS roughness values for the different LDHs layers smaller than 1 nm. The roughness and the thickness of the deposited layer can be reduced by increasing the rotational speed of the spin-coater.

3.3.2 Hybrid ODN/LDH biomembrane morphology

In order to confirm the hypothesis of the correct functionalization of the LDHs with ODN-5'NH_2, we characterised the morphology of the different biomembranes on each preparation step.

It can be observed the appearance of furrows of about 1.5-2.5 nm in width and maximum of 8.55 nm in high on each of the LDHs functionalized with ODN-5'NH_2, as shown in Figure 5.b which demonstrate the successful transfer of the ODN on the LDH substrate. After the

hybridization of the ODN probes with their complementary 100 bases, the profile image of the biomembranes after the hybridization shows a structure of about 30-35 nm in high (Figure 5.c). This corresponds to the size of a sequence of 100 bases extended and we can conclude about the conformation of the immobilized ODN probe that is very favourable for the hybridization with its complementary in vertical arrangement to the surface.

3.4 Characterization of the DNA sensor

3.4.1 Electrochemical Impedance Spectroscopy

The preparation of the DNA sensor consists in the hybridization of the DNA probes of 100 bases for a selective molecular recognition of the remaining 80 bases of a given target. For this, we used DNA probes of 100 bases chemically synthesized. The first 20 bases were complementary to the ODN probes immobilized on the modified LDH-based electrodes. Figures 6 shows the Nyquist diagram of the hybridization of 100 up complementary sequence (Figure 6.a) and the variation in the impedance as a function of the concentration of target probe of complementary (100 up) and non complementary (NC100) 100 base sequences to saturation (Figure 6.b). The saturation in the sensor response is obtained for a concentration of 270 ng/ml respectively 180 ng/ml, in host matrix of Mg_2AlCO_3 respectively Mg_3AlCO_3. These value corresponding to the recovery rate of probes into the surface that should be higher for Mg_2Al. We can conclude that from a concentration of 270 ng/ml, all the immobilized ODN probes (NH_2-20 down) in the Mg_2Al LDH matrix were hybridized with the complementary strand of 100 bases target probe (100 up). Also we can conclude that this hybridization is highly specific as the addition of increasing amounts of a non complementary 100 bases sequence (100 NC) did not produce any relevant electrical response in the sensor up to 270 ng/ml (Figure 6.b).

3.4.2 Response, Selectivity and Reusability of the DNA sensor

The Nyquist diagram of the sensor response based on ODN/Mg_2AlCO_3 to various concentrations of complementary DNA sequence 80 down is shown in Figure 7.a. The equivalent electric circuit corresponding to the sensor built for the determination of DNA probe of 80 bases (80 down) is shown in Figure 7.b. R_{ct} represents the charge transfer resistance associated with the electrolyte, R_1 and CPE_1 are the charge transfer resistance and the constant charge element of the electrode/electrolyte interface, respectively. R_2 and CPE_2 represent the charge transfer resistance and the constant charge element of the ODN/electrode interface, respectively.

The formula (A1) of total impedance of the modified electrode is then written as

$$Z_{tot}=Z_{Re}+Z_{Im}=R_{ct}+[R_1//CPE_1]+[R_2//CPE_2] \quad (A1)$$

With $Z_{CPE}= 1/Q(if/2\pi)^{n1}$, where Q (F/cm²) and n correspond to CPE parameters and f is the frequency

Table 1 summarizes the parameters of the equivalent circuit of DNA-sensor, which allows us to conclude about the nature of the response which is due to diffusion phenomena at the sensor interface/electrolyte and on the stability of the hybrid biomembrane.

The R_1 resistance increases from 80.951 kΩ to 112.700 kΩ before and after hybridization with the 100 base complementary DNA sequence (100 up) (for a concentration of 300 ng/ml). This reflects the insulating nature of the 20 down/100 up DNA hybrid molecule. On the other side, the constant phase element (CPE_1) decreases reflecting an increase in the thickness of the surface layer. Finally, the variations in the equivalent circuit ($R_2//CPE_2$) associated with

the ODN/LDH interface of the CPE_2 is related to the decrease in the porosity of the membrane.

Table 1: Values obtained for the equivalent circuit components measured at 65 ° C.

c(ng/ml)	$R_{ct}(\Omega)$	$R_1(\Omega)$	Q_1 ($F.cm^{-2}$)	n_1	$R_2(\Omega)$	$Q_2(F.cm^{-2})$	n_2
5'NH_2-ODN	135	26948	4.3445E-5	0.889	6324	8.5962E-8	0.935
100 bases complementary DNA							
3	135	80951	3.8022E-5	0.898	15843	6.839E-8	0.965
300	135	112700	3.6468E-5	0.904	14808	6.6937E-8	0.967
Complementary 80down DNA							
0	135	112700	3.6468E-5	0.904	14808	6.6937E-8	0.967
1.8	135	134790	3.5840E-5	0.903	14873	6.7578E-8	0.966
18	135	160750	3.4983E-5	0.906	14710	6.868E-8	0.964
90	135	178830	3.4438E-5	0.910	14480	7.0236E-8	0.916
180	135	199070	3.3994E-5	0.910	11871	6.8291E-8	0.964
270	135	221290	3.3671E-5	0.909	12034	6.6358E-8	0.968

As shown in figure 7.c, the calibration curve related to the hybridizatrion of the complementary 80 down DNA sequence at 65 °C show a linear variation of the charge transfer resistance R_1 for concentrations ranging from 18 ng/ml to 270 ng/ml. This impedance variation reflects the sensitivity of the DNA-biosensor was 286.7 Ω/[ng/ml] with a correlation coefficient R^2=0.999. The detection limit was lower than 1.8 ng/ml (7 10^{-11} M). The results are very interesting since they are of the same order of magnitude as those of conventional techniques such as ELISA or biomarkers.

The selectivity measurements of the sensor performed to verify the validity of the previous results and the specificity of the measurement were performed under the same experimental conditions as those described above. In these experiments a negative control oligonucleotide (100 NC) was used instead of the 100 up sequence. No significant variation in the different impedances of the sensor was obtained showing the high degree of selectivity obtained with the sensor.

In addition we have made up to 10 consecutive measurements of the electrical response after regeneration of the sample and the calibration curves were similar in shape and in sensitivity (±7 %, data not shown).

Finally, the characteristics of the sensor sensitivity to the hybridization of the target DNA were performed at two temperatures (65 and 37 °C). The variation of R_1 measured with the temperature was quite similar in shape and in order (sensitivity of 286.7 respectively 238.5 Ω/ng.ml^{-1}) indicating that significant sensitivity was obtained either at optimal hybridization reaction (65 °C) or at physiological conditions (37 ºC). This data indicates that the LDH-based DNA–biosensor can be used at several temperature conditions without lost of performance. This is important in order to build DNA sensors for the analysis of single mutations in DNA as the stringency conditions should be optimized for each DNA sequence in order to achieve the best discrimination between perfect match and mutated sequences. Work in these directions is currently being done and results will be presented in due course.

4. Conclusions and Perspectives

The study that we conducted in order to develop DNA sensors by self-assembly on thin films of LDH shows that the immobilization protocol is well suited for the anchoring of DNA

probes in a vertical conformation which favours hybridization as shown in the AFM measurements. Therefore, we validated this methodology for the development of DNA sensors presenting very competitive characteristics compared to those techniques currently used in clinical laboratories. The linear range is very wide, from 18 to 270 ng/ml and the limit of detection is very interesting for the preventive screening of diseases. Finally, the type of sensor described in this study improves current techniques regarding the speed of response (less than 10 minutes), ease of implementation, its reproducibility and the ability to reuse the sensor several times.

Acknowledgements:

This work was supported by the Spanish MICINN (CTQ2010-20541), the Generalitat de Catalunya (2009/SGR/208) and CIBER-BBN. Special funds were obtained from Spanish and Tunisian government to support this work within AECID program (A/2675/05 and A/6256/06).

Figures Captions:

Figure 1: Scheme of the protocol used in this study for the preparation of hybrid ODN/LDHs.

Figure 2: PXRD diffractograms of LDHs.

Figure 3: IR spectra of the LDHs with and without 20bases probe with amino DNA.

Figure 4: Influence of the functional group of the ODN-5' end in the immobilization. IR spectra of LDHs functionalized with unmodified, 5'-thiol and 5'-amino-oligonucleotides. Clear DNA signals are observed with the 5'-amino-oligonucleotides indicating a more efficient functionalization of LDHs membranes. 1) 3400-3200 cm^{-1} wide band corresponding to amino and hydroxyl groups, 2) 2950 and 3) 2850 cm^{-1} amino, hydroxyl and C-H stretching, 4) 1650 cm^{-1}, 5) 1600 cm^{-1}, 6) 1450 cm^{-1} and 7) 1400 cm^{-1} C=O, C=N, C=C stretching, 8) 1350 cm^{-1} and 1050 cm^{-1} aromatic and P-O bands.

Figures 5: 3D AFM topography image of LDH and DNA/LDHs biomembranes. a) Initial deposited Mg_2AlCO_3 LDH layer. b) NH_2- 20 down oligonucleotide/ Mg_2AlCO_3 biomembranes before hybridization with the complementary DNA 100 bases (100 up). c) after hybridization with the complementary DNA 100 bases (100 up).

Figures 6: a) Nyquist diagram of the DNA sensor of DNA at 65 °C for the recognition of the complementary 100 bases sequence (100 up) (ODN/Mg_2AlCO_3 membrane). b) Variation in

the impedance as a function of the concentration of a complementary 100 bases sequence (100 up) or a non complementary 100 bases sequence (100 NC).

Figures 7: Characteristics of the sensor to the hybridization of the DNA sequence (80 down) at 65 °C. a) Nyquist diagram. b) Equivalent circuit of the DNA biosensor. c) Variation in the impedance as a function of the concentration of complementary 80 down sequence (calibration curve). The membrane (Mg_2AlCO_3) used was functionalized with the NH_2-20 down sequence and hybridized with the 100 up sequence before the detection of the 80 down DNA sequence.

Figure 1:

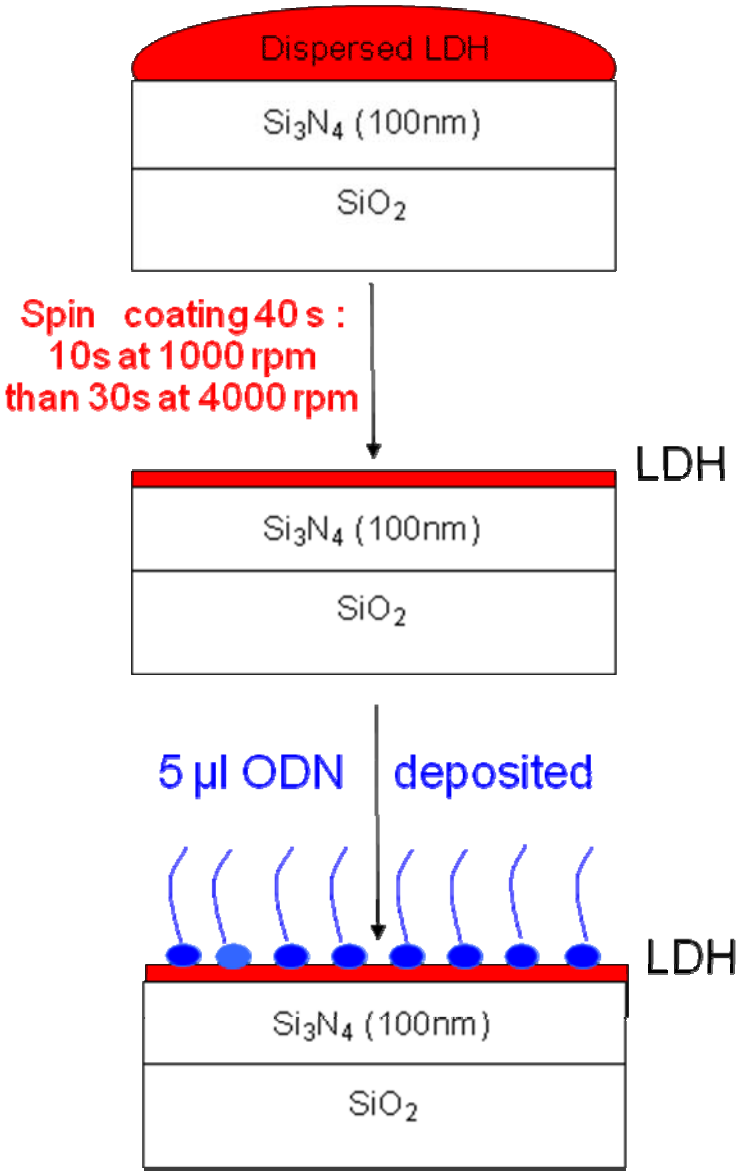
Dispersed LDH
Si_3N_4 (100nm)
SiO_2
Spin coating 40 s :
10s at 1000 rpm
than 30s at 4000 rpm
LDH
Si_3N_4 (100nm)
SiO_2
5 µl ODN deposited
LDH
Si_3N_4 (100nm)
SiO_2

Figure 2:

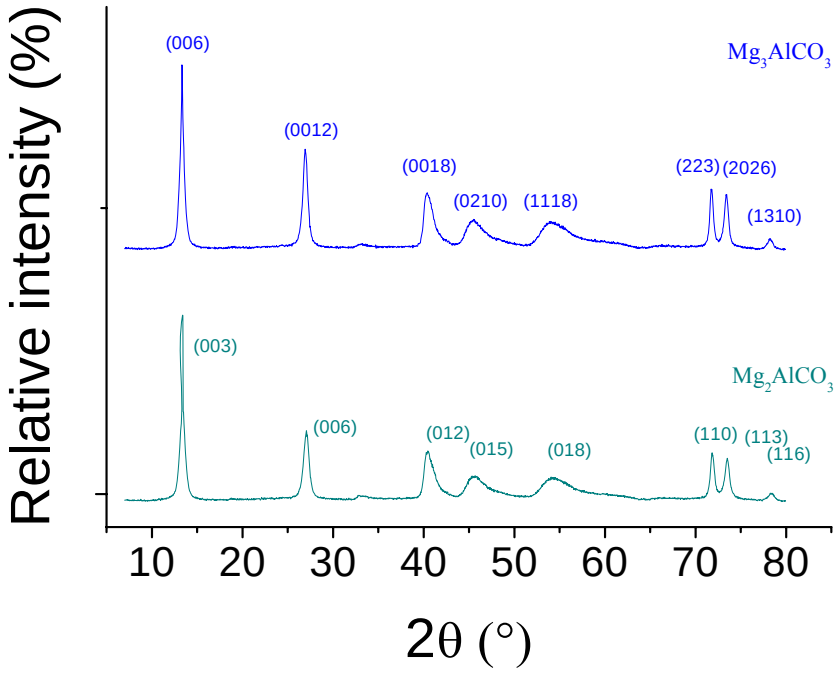
Relative intensity (%)
(006)
(0012)
(0018)
(0210)
(1118)
(223)
(2026)
(1310)
Mg3AlCO3
(003)
(006)
(012)
(015)
(018)
(110)
(113)
(116)
Mg2AlCO3
10
20
30
40
50
60
70
80
2θ (°)

Figure 3:

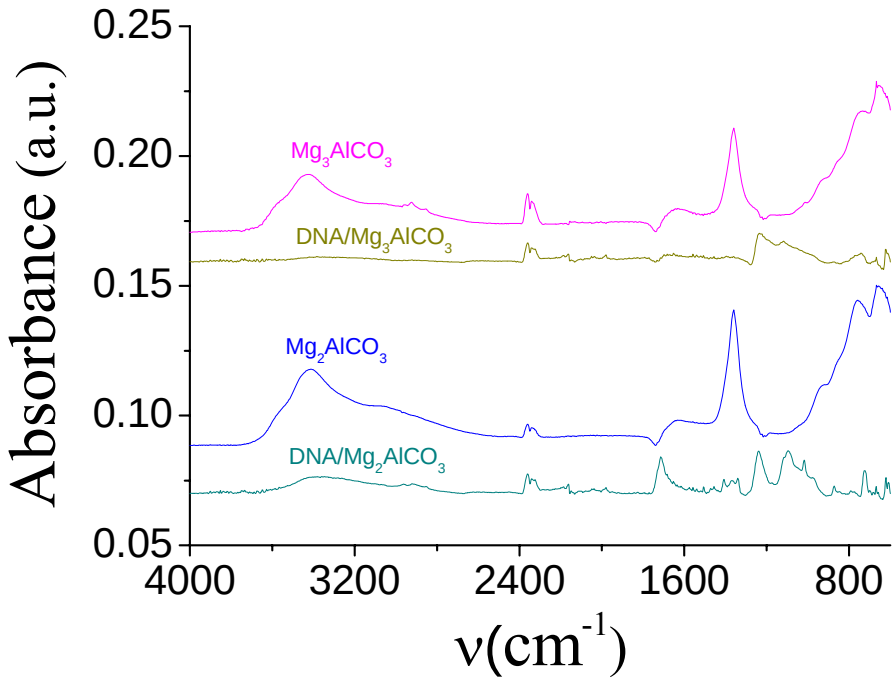
Absorbance (a.u.)
0.25
0.20
0.15
0.10
0.05
4000
3200
2400
1600
800
ν(cm-1)
Mg3AlCO3
DNA/Mg3AlCO3
Mg2AlCO3
DNA/Mg2AlCO3

Figure 4:

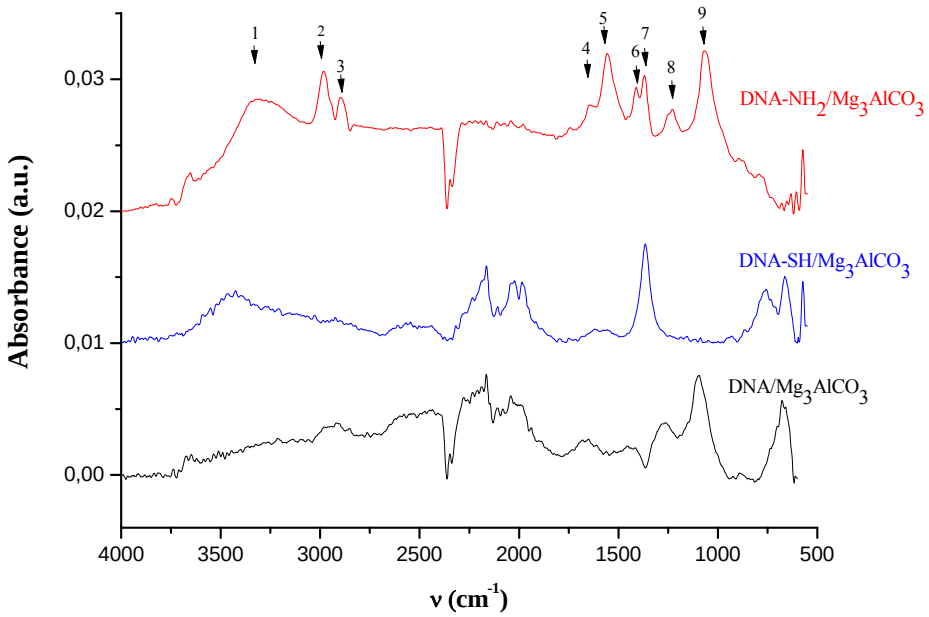
1
2
3
4
5
6
7
8
9
0,03
0,02
0,01
0,00
Absorbance (a.u.)
DNA-NH2/Mg3AlCO3
DNA-SH/Mg3AlCO3
DNA/Mg3AlCO3
4000
3500
3000
2500
2000
1500
1000
500
ν (cm-1)

Figures 5:

a)

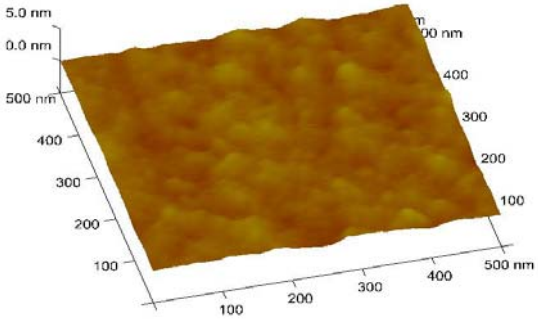

b)

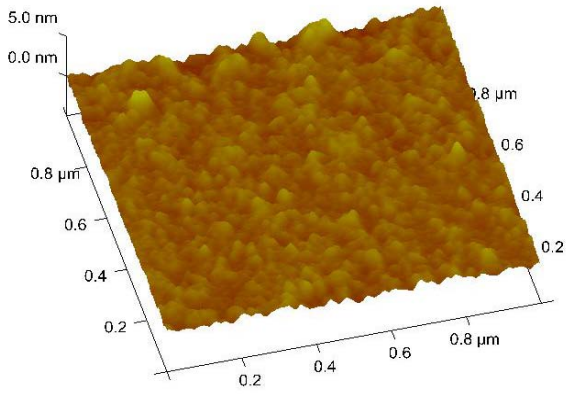

c)

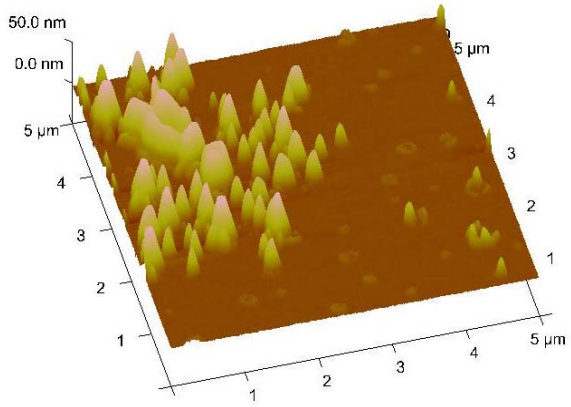

Figures 6 :

a)

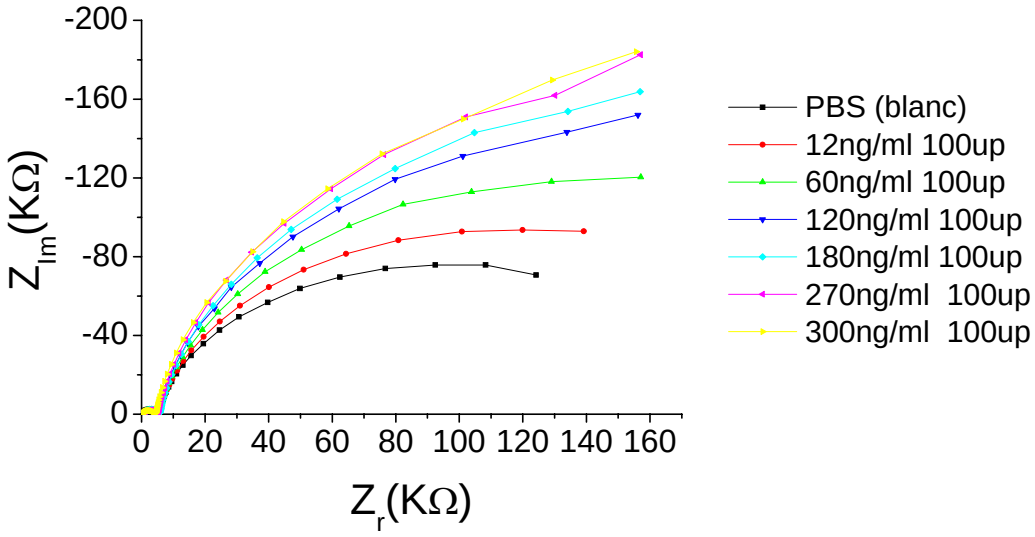
-200
-160
-120
-80
-40
0
0 20 40 60 80 100 120 140 160
Z_Im(KΩ)
Z_r(KΩ)
PBS (blanc)
12ng/ml 100up
60ng/ml 100up
120ng/ml 100up
180ng/ml 100up
270ng/ml 100up
300ng/ml 100up

b)

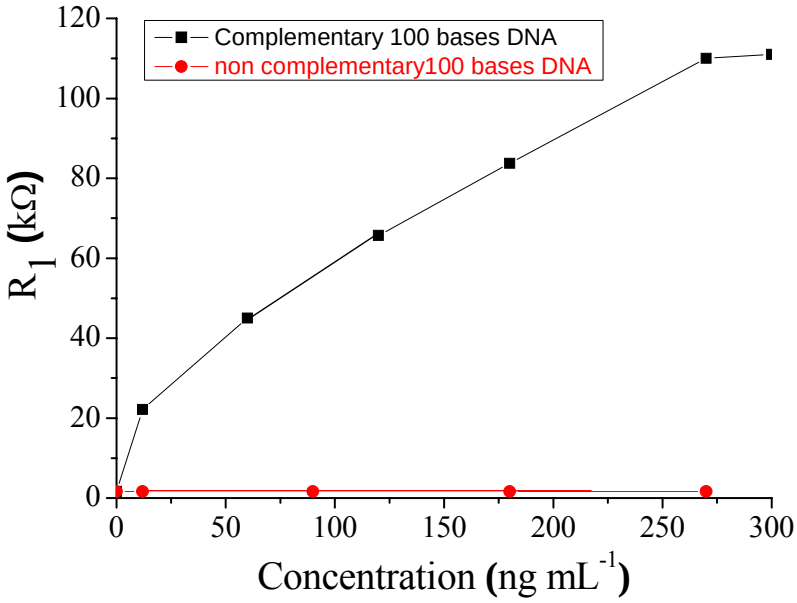
120
100
80
60
40
20
0
0 50 100 150 200 250 300
R_1 (kΩ)
Concentration (ng mL^-1)
Complementary 100 bases DNA
non complementary100 bases DNA

Figures 7 :

a)

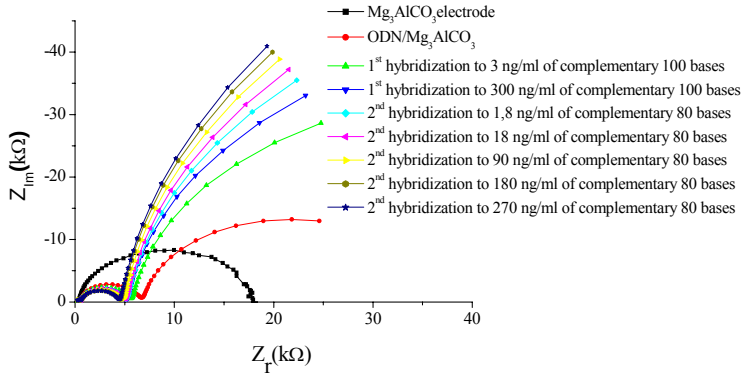

b)

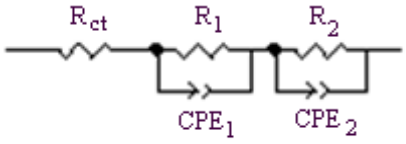

c)

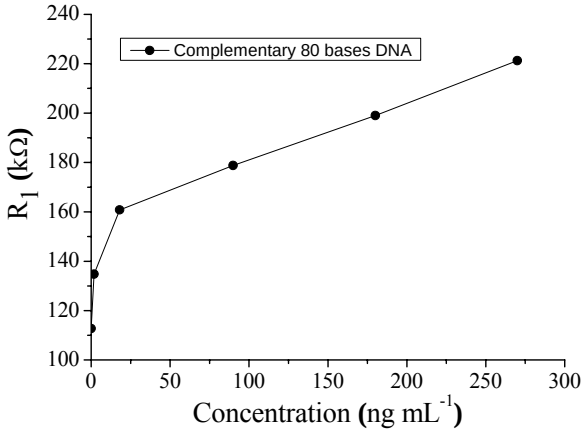

References

[1] D. Samanta, A. Sarkar, Immobilization of bio-macromolecules on self-assembled monolayers: methods and sensor applications. Chem. Soc. Rev. 40 (2011) 2567-2592.

[2] E.H. Lan, B. Dunn, J.I. Zink, Nanostructured systems for biological materials. Methods Mol. Biol. 300 (2005) 53-79.

[3] D.G. Evans, X. Duan, Preparation of layered double hydroxides and their applications as additive in polymers, as precursors to magnetic materials and in biology and medicine. Chem. Comm. 7 (2006) 485-496.

[4] A.I. Khan, D.J. O'Hare, Intercalation chemistry of layered double hydroxides: recent developments and applications. J. Mater. Chem. 12 (2002) 3191–3198.

[5] A.M. Fogg, V.M. Greeen, H.G. Harvey, D. O'Hare New separation science using shape-selective ion exchange intercalation chemistry. Adv. Mater. 11 (1999) 1466–1469.

[6] P. Beaudot, M.E. De Roy, J.P. Besse, Preparation and characterization of intercalation compounds of layered double hydroxides with metallic oxalato complexes. Chem. Mater. 16 (2004) 935–945.

[7] B.F.Sels, D.E. De Vos, P.A. Jacobs, Bromide-assisted oxidation of substituted phenols with hydrogen peroxide to the corresponding p-quinol and p-quinol ethers over WO4(2-)-exchanged layered double hydroxides. Angew. Chem. Int. Ed. 44 (2004) 310-313

[8] J.-H. Choy, S.-Y. Kwak, J.S. Park, Y.-J. Jeong, J. Portier, Intercalative nanohybrid of nucleoside monophosphates and DNA in layered metal oxide, J. Am. Chem. Soc. 121 (1999) 1399-1400

[9] J.-H.Choy, S.-Y Kwak, J.S. Park, Y.-J. Jeong, Cellular uptake behavior of [gamma P-32] labeled ATP-LDH nanohybrid. J. Mater. Chem. 11 (2001) 1671-1674.

[10] T. Itoh, T. Shichi, T. Yui, H. Takahashi, Y. Inui, K. Takagi, Reversible color changes in lamella hybrids of poly(diacetylenecarboxylates) incorporated in layered double hydroxide nanosheets. J. Phys. Chem. B 109 (2005) 3199-3206.

[11] J.A. Gursky, S.D. Blough, C. Luna, C. Gomez, A.N. Luevano, Gardner E.A. Particle-particle interactions between layered double hydroxide nanoparticles. J. Am. Chem. Soc. 128 (2006) 8376-8377

[12] L.Mohanambe, S. Vasudevan, Anionic clays containing anti-inflammatory drug molecules: comparison of molecular dynamics simulation and measurements. J. Phys. Chem. B 109 (2005) 15651-15658

[13] Z. Liu, R. Ma, M. Osada, N. Iyi, Y. Ebina, K. Takada, T. Sasaki, Synthesis, Anion Exchange, and Delamination of Co−Al Layered Double Hydroxide: Assembly of the Exfoliated Nanosheet/Polyanion Composite Films and Magneto-Optical Studies J. Am. Chem. Soc.128 (2006) 4872-4880;

[14] H. Chen, F. Zhang, S. Fu, X. Duan, In□Situ Microstructure Control of Oriented Layered Double Hydroxide Monolayer Films with Curved Hexagonal Crystals as Superhydrophobic Materials. Adv. Mater. 18 (2006) 3089-3093

[15] J.H. Lee, S. Rhee, D.-Y. Jung, Selective Layer Reaction of Layer-by-Layer Assembled Layered Double-Hydroxide Nanocrystals. J. Am. Chem. Soc. 129 (2007) 3522-3523.

[16] J.H. Lee, Y. Du and D. O'Hare, Growth of Oriented Thin Films of Intercalated α-Cobalt Hydroxide on Functionalized Au and Si Substrates. Chem. Mater. 21 (2009) 963-968

[17] S. Hidouri, Z.M. Baccar, H. Abdelmelek, T. Noguer, J.-L. Marty and M. Campàs, Structural and functional characterisation of a biohybrid material based on acetylcholinesterase and layered double hydroxides. Talanta 85 (2011) 1882-1887

[18] Z.M. Baccar, I. Hafaiedh, Immobilization of HRP Enzyme on layered double hydroxides for Biosensor Application. International Journal of Electrochemistry (2011) DOI: 10.4061/2011/934893.

[19] Z. M. Baccar, D. Caballero, N. Zine, N. Jaffrezic-Renault, and A. Errachid, Development of Urease/Layered Double Hydroxides Nanohybrid Materials for the Urea Detection: Synthesis, Analytical and Catalytic Characterizations. Sensor lett. 7 (2009) 647-655

[20] Z.M. Baccar, S. Hidouri, A. Errachid, O. Ruiz-Sanchez, Study of bi-enzyme immobilization onto LDH nanomaterials for histamine biosensor application. J. Nanosci. Nanotechnol. 11 (2011) 8798-8803

[21] S. Cosnier, P. Mailley, Recent advances in DNA sensors. Analyst 133 (2008) 984-991

[22] S.D. Keighley, P. Li, P. Estrela, P. Migliorato, Optimization of DNA immobilization on gold electrodes for label-free detection by electrochemical impedance spectroscopy. Biosensors & Bioelectronics 23 (2008) 1291-1297.

[23] S.D. Keighley, P. Estrela, , P. Li, P. Migliorato, Optimization of label-free DNA detection with electrochemical impedance spectroscopy using PNA probes. Biosensors & Bioelectronics 24 (2008) 906-911.

[24] A. Kukol, P. Li, P. Estrela, P. Ko-Ferrigno, P. Migliorato, Label-free electrical detection of DNA hybridization for the example of influenza virus gene sequences. Anal. Biochem. 374 (2008) 143-153.

[25] A. Ongaro, F. Griffin, L. Nagle, D. Iacopino, R. Eritja, D. Fitzmaurice, DNA templated assembly of a protein-functionalized nanogap electrode. Adv. Mat. 16 (2004) 1800-1803

[26] Miyata S. The Syntheses of Hydrotalcite-Like Com- pounds and Their Structures and Physico-Chemical Properties I: The Systems Mg^{2+}-Al^{3+}-NO_3^-, Mg^{2+}-Al^{3+}-Cl^-, Mg^{2+}-Al^{3+}-ClO_4^-, Ni^{2+}-Al^{3+}-Cl^- and Zn^{2+}-Al^{3+}-Cl^-. Clay Miner. 1975, 23, 369-375.

[27] G.J. Ross and H. Kodama, Properties of a synthetic magnesium-aluminum carbonate hydroxide and its relationship to magnesium-aluminum double hydroxide, manasseite and hydrotalcite. Am. Mineral. 52 (1967) 1036-1047 .

[28] M. Bellotto, B. Rebours, O. Clause, J. Lynch, D. Bazin, and E. Elkaim, A Reexamination of Hydrotalcite Crystal Chemistry. J. Phys. Chem. 100 (1996) 8527-8534.

[29] Y. You, H.T. Zhao, and G.F. Vance, Adsorption of dicamba (3,6-dichloro-2-methoxy benzoic acid) in aqueous solution by calcined–layered double hydroxide. Appl. Clay Sci. 21 (2002) 217-226.

[30] V.R.L. Constantino and T.J. Pinnavaia, Basic properties of Mg2+1-x Al3+x layered double hydroxides intercalated by carbonates, hydroxide, chloride, and sulfate anions. Inorg. Chem. 34 (1995) 883-892.